APPLICATIONS OF
MODELLING AND SIMULATION
http://arqiipubl.com/ams eISSN 2600-8084 VOL 9, 2025, 227-240

Probabilistic Fatigue Life Prediction of Plain Concrete Under Cyclic Loading Through Experimental Finite Element and Stochastic Modelling

Mohamad Shazwan Ahmad Shah*, Sarehati Umar, Nurul 'Azizah Mukhlas, Ng Chiew Teng, Haikhal Faeez Hairuddin, Wan Ikram Wajdee Wan Ahmad Kamal, Hanis Hazirah Arifin and Norhazilan Md. Noor

Department of Structure and Materials, Faculty of Civil Engineering, Universiti Teknologi Malaysia, 81310 UTM Johor Bahru, Johor, Malaysia

*Corresponding author: mohamadshazwan@utm.my

Submitted 13 March 2025; Revised 10 April 2025; Accepted 03 May 2025; Available online 07 June 2025.

Abstract: The fatigue failure of plain concrete under cyclic loading remains a challenge in structural engineering, particularly for infrastructure exposed to repeated stress fluctuations. Existing fatigue life prediction models fail to fully capture material variability and uncertainties, leading to inconsistent estimations and potential structural failures. This study develops a probabilistic finite element model to predict the fatigue life of plain concrete beams under cyclic loading. Fourteen data points from experimental tests and numerical simulations were analysed, incorporating probabilistic methods to enhance predictive accuracy. Fatigue behaviour was characterized through stress–life (S–N) curves, and regression analysis established the fatigue life equation. The integration of exponential distribution models enabled probabilistic fatigue life estimation across stress levels and failure probabilities. The methodology involves finite element simulation with validated mesh convergence, integration of experimental fatigue data, and application of exponential probability distribution for multi-probability failure predictions. This study directly supports SDG 9 by promoting resilient infrastructure through advanced fatigue life prediction techniques, enhancing the durability and serviceability of concrete structures under cyclic loading. Additionally, mesh convergence validation ensured computational accuracy, identifying an optimal mesh size for reliable numerical simulations. The final logarithmic S–N curve exhibited a high correlation coefficient (R^2 = 0.989) between experimental and simulated data. The results underscore the importance of integrating deterministic finite element methods with probabilistic modelling to achieve a robust reliable fatigue life prediction framework for concrete structures. This research advances understanding of fatigue performance in plain concrete, providing essential insights for enhancing infrastructure durability and reliability.

Keywords: Failure probability; Finite element analysis; High-cycle fatigue; Probabilistic fatigue; S–N curve.

1. INTRODUCTION

Fatigue failure in concrete structures poses a critical threat to infrastructure integrity, particularly in applications such as bridge decks, wind turbine towers, railway sleepers, and pavements, where cyclic loading is unavoidable [1]. Unlike ductile materials, concrete exhibits quasi-brittle behaviour, meaning that microstructural degradation under fatigue is progressive and irreversible, often leading to unexpected structural failures. While fatigue failure mechanisms in concrete have been studied for decades [2], the lack of a universally accepted fatigue life prediction model for plain concrete underscores the complexity of the problem. Fatigue damage depends on numerous factors, including material heterogeneity, environmental conditions, and complex loading histories, making accurate fatigue life prediction exceptionally challenging [3].

The current methodologies for assessing fatigue life in concrete structures primarily rely on deterministic approaches, such as traditional stress–life (S–N) curves and fracture mechanics, which assume material properties and loading conditions to be uniform and predictable. However, these methods fail to account for the inherent stochastic nature of concrete, leading to significant uncertainties in fatigue life estimations [4]. Recent studies have attempted to bridge this gap through machine learning techniques, such as artificial neural networks (ANNs), and probabilistic methods, including Bayesian inference and Monte Carlo simulations [5]. These emerging approaches have demonstrated improved accuracy, but they lack the integration of finite element modelling for enhanced reliability.

To address these challenges, this research develops a probabilistic finite element model for predicting the fatigue life of plain concrete under cyclic loading. By combining experimental validation, numerical modelling, and statistical analysis, this study provides a comprehensive framework that overcomes the limitations of purely deterministic methods. The model

incorporates finite element simulations in Abaqus, validated through mesh convergence studies and regression-based S–N curve fitting to ensure computational accuracy. Additionally, a probabilistic approach is applied to estimate the number of cycles to failure at various stress levels and confidence intervals. By integrating deterministic and probabilistic methodologies, this study significantly advances fatigue life prediction, with direct implications for structural reliability, safety assessment, and cost-effective maintenance strategies in concrete infrastructure.

Fatigue failure in plain concrete remains one of the most underestimated yet critical challenges in structural engineering. Despite extensive research, current fatigue life prediction models suffer from inherent limitations, primarily due to their reliance on deterministic methodologies that fail to capture the stochastic variability of concrete materials and loading conditions [6]. Conventional approaches, including empirical S–N curve analysis and fracture mechanics models, assume that material behaviour follows a fixed deterministic path, ignoring the effects of microstructural heterogeneity, environmental fluctuations, and load sequence effects [1, 7]. This can lead to highly inconsistent fatigue life predictions, premature failures, and excessive safety margins in structural design.

Another significant limitation of current fatigue prediction models is the scarcity of high-quality fatigue data, as concrete fatigue experiments are time-consuming and expensive [8]. This data limitation further restricts the applicability of machine-learning-based approaches, such as ANNs, which require large datasets for robust training and validation [1]. Consequently, a more effective approach is required – one that integrates experimental data, numerical simulations, and probabilistic analysis to provide a comprehensive and reliable fatigue life prediction framework.

This study addresses these gaps by developing a probabilistic finite element model for fatigue life prediction, combining experimental fatigue testing with numerical simulations in Abaqus and probabilistic modelling. The mesh sensitivity of the finite element models is critically evaluated to ensure numerical accuracy, with exponential probability distributions applied to estimate fatigue life under varied stress levels and probability thresholds. Unlike previous studies, which either relied on deterministic models or isolated probabilistic approaches, this study synergizes both methodologies, creating a hybrid predictive model that is computationally efficient and statistically robust. The research findings provide critical insights for engineers, researchers, and industry professionals, enabling the development of more reliable, cost-effective, and resilient fatigue design strategies for plain concrete structures.

2. LITERATURE REVIEW

2.1 Fatigue Failure Mechanisms in Plain Concrete

Fatigue failure in plain concrete is a highly complex and progressive phenomenon characterized by internal microcrack accumulation, gradual stiffness and strength reduction, and eventual structural failure [9]. Unlike static loading conditions, where failure occurs under a single peak stress event, fatigue damage in concrete is induced by cyclic loading, which gradually deteriorates the material at a microstructural level [10]. A three-phase process of fatigue failure – microcrack initiation, crack propagation, and final structural breakdown has been identified, with the quasi-brittle nature of concrete accelerating this degradation under cyclic stresses. Studies have demonstrated that stress fluctuations significantly impact the longevity of concrete structures, particularly in cases where environmental conditions, loading histories, and material properties introduce variability [10].

A critical challenge in fatigue life prediction is the heterogeneous composition of concrete, which inherently contains voids, microcracks, and aggregate–matrix interfaces that act as stress concentrators and influence crack nucleation and growth [11]. Fatigue behavior in concrete is often modeled using the classical stress-life (*S*-*N*) power law, expressed as $S = aN^b$, where S is the applied stress amplitude, N is the number of cycles to failure, and a, b are empirically determined material constants. However, due to the inherent variability of concrete, deterministic *S*-*N* models often fail to capture the scatter observed in experimental fatigue data. Additionally, environmental conditions such as temperature fluctuations and humidity exacerbate crack propagation, further reducing fatigue life [12]. Given these complexities, traditional fatigue prediction models fail to provide a universal, high-accuracy approach, necessitating a multifaceted methodology that integrates experimental, numerical, and probabilistic techniques.

2.2 Influence of Material and Loading Factors on Fatigue Life

Concrete fatigue performance is highly sensitive to material properties, loading conditions, and environmental influences. Compressive and tensile strength, aggregate size, porosity, and ultimate strain are key factors that dictate fatigue resistance [13]. Smaller aggregate sizes (10 mm) tend to improve fatigue performance at lower stresses by enhancing packing density and reducing microcrack initiation [14]. Additionally, the water–cement ratio plays a crucial role, as excessive water content increases porosity and weakens the cement matrix, making the concrete more susceptible to cyclic-stress-induced damage [6].

Cyclic loading characteristics, particularly stress range, frequency, and load amplitude, directly impact fatigue life. Higher stress levels significantly reduce fatigue resistance, with some findings suggesting that stress amplitudes exceeding 60% of the ultimate strength can greatly reduce fatigue life [10]. Moreover, variable-amplitude loading introduces complexity, as repeated load fluctuations lead to progressive stiffness degradation and nonlinear crack propagation [15]. These findings highlight the need for fatigue models that integrate deterministic and probabilistic influences, improving prediction accuracy and enabling realistic failure estimations under diverse loading scenarios.

2.3 Existing Approaches to Failure Life Prediction

Several methodologies have been developed to predict concrete fatigue life, ranging from traditional S–N curves to advanced computational and probabilistic approaches. The S–N curve method, widely used in fatigue studies, establishes a power-law relationship between stress amplitude and number of cycles to failure. However, this approach is purely empirical and fails to

capture variability in material properties, environmental effects, and load history, leading to inconsistent predictions [16]. Fracture mechanics models, which focus on crack propagation under cyclic loading, are a more fundamental approach but often require extensive experimental calibration and computational resources [17]. For cumulative damage, Miner's Rule is often applied, expressed as $D = \sum (n_i/N_i)$ assuming linear damage accumulation without considering load interaction effects. While these deterministic models are useful for simplified analysis, they do not capture the probabilistic nature of fatigue failure, which can be described using statistical distributions such as the exponential or Weibull models.

Recent advances in finite element analysis (FEA) have improved fatigue prediction accuracy by simulating crack propagation, stress distribution, and damage evolution in concrete structures [18]. Finite element models incorporating the concrete damage plasticity model have shown promise in predicting fatigue behaviour under various loading conditions, particularly when combined with experimental validation and sensitivity analyses [19]. Additionally, scaled boundary finite element methods have been employed for modelling cyclic crack propagation, improving computational efficiency and geometric adaptability [20]. However, despite enhancing predictive accuracy, these models still rely on deterministic assumptions, limiting their applicability in real-world structural conditions.

2.4 Role of Probabilistic Methods in Fatigue Life Prediction

Given the stochastic nature of fatigue failure, probabilistic approaches have emerged as critical tools for improving fatigue life prediction in concrete structures. Monte Carlo simulations, for example, utilize stochastic sampling to model fatigue strength uncertainties and generate synthetic datasets for statistical evaluation [21]. Applied in offshore wind turbine foundations and bridge structures, these methods provide sensitivity and reliability assessments that traditional deterministic models lack [22]. Additionally, Bayesian regularization in neural networks is effective in mitigating overfitting and refining fatigue life estimations, particularly for tensile fatigue prediction in concrete structures [1].

Recent studies have also integrated Markov chain Monte Carlo methods to refine damage prediction models, enhancing accuracy in corrosion-fatigue crack assessments [23]. For example, Wu et al. applied Bayesian inference to predict the fatigue life of reinforced concrete beams, incorporating chloride-induced corrosion effects [24]. Similarly, Lee et al. used the Metropolis-Hastings algorithm to improve efficiency in estimating sectional-area probabilities, advancing fatigue reliability assessments of prestressed concrete bridges [25]. Weibull-distribution-based fatigue analysis is also effective for modelling material degradation and failure probabilities under cyclic loading [26]. In stochastic modeling, fatigue life N is often assumed to follow either a log-normal or exponential distribution, as adopted in this study. The exponential distribution is defined by $f(N) = \lambda e^{-\lambda N}$, where λ is the rate parameter.

Despite the success of these probabilistic methods, their integration with finite element modelling is still limited. Many existing probabilistic fatigue models are data-driven and empirical, lacking the capability to physically simulate fatigue behaviour at a microstructural level. This gap highlights the urgent need for a hybrid approach that combines FEA with probabilistic modelling, ensuring both numerical accuracy and statistical robustness in fatigue life predictions.

2.5 Research Gap and Need for Hybrid Approach

A critical limitation of existing fatigue life prediction models is the lack of integration between deterministic FEA and probabilistic methods. While FEA-based models offer detailed insights into stress distribution and crack propagation, they fail to account for random material defects and environmental uncertainties. Conversely, probabilistic approaches provide uncertainty quantification and statistical reliability but lack mechanistic accuracy in predicting fatigue damage evolution. No existing research provides a unified framework that effectively incorporates both deterministic and stochastic perspectives, leading to discrepancies between theoretical predictions and real-world structural performance.

This study addresses this gap by developing a probabilistic finite element model for concrete fatigue life prediction. It integrates numerical simulations using Abaqus, validated through mesh convergence analysis, with probabilistic modelling techniques such as exponential distribution analysis. By combining these methodologies, the research aims to overcome the limitations of purely deterministic models, enhance prediction accuracy, and provide a comprehensive fatigue life estimation framework with computational precision that also incorporates statistical variability. This hybrid approach is crucial for improving structural reliability, optimizing design parameters, and minimizing premature failures in concrete infrastructure.

3. METHODOLOGY

This study involved three key activities: construction of the S–N curve, development and validation of a finite element model using Abaqus, and enhancement of the S–N curve using probabilistic models.

3.1 Construction of S–N Curve

In this study, the S–N curve for plain concrete was constructed using experimental data. A concrete beam with a water–cement ratio of 0.4 and dimensions of 1065 mm × 110 mm × 100 mm was used. The average ultimate flexural strength under static loading was determined to be 6.53 MPa. The beam was subjected to cyclic loading at a fixed frequency of 30 Hz with maximum flexural stresses of 4.870, 4.568, 4.497, 3.997, 3.426, and 2.286 MPa, representing 74.6%, 70.0%, 68.9%, 61.2%, 52.5%, and 35.0% of the ultimate strength, respectively. The number of cycles to failure was recorded for each stress level to construct the S–N curve. The experimental fatigue data adopted in this study were obtained from [27], where plain concrete beams were tested under controlled three-point bending conditions at various stress levels. The key testing parameters and data have been extracted and integrated into this probabilistic modeling framework. For detailed test setup, instrumentation, and procedures, readers are referred to the original study. The applied stress levels: 35%, 52.5%, 61.2%, 68.9%, 70%, and 74.6% of the ultimate flexural strength were chosen to span the high-cycle fatigue (long-life, low-stress) and low-cycle fatigue (short-life, high-

stress) regimes. This range is widely adopted in concrete fatigue research [27] and is consistent with expected stress amplitudes in service conditions of structural elements such as bridge decks, pavements, and offshore substructures. The ultimate flexural strength was established through static three-point bending tests on plain concrete beams, yielding a reference value of 6.53 MPa [27]. Each experimental fatigue test was conducted as a percentage of this static value, as summarized in Table 1.

3.2 Development and Validation of Finite Element Model Using Abaqus

The behaviour of a plain concrete beam was modelled and analysed using Abaqus software following several systematic steps:

Part Creation. A deformable solid part with an extrusion shape was created in a 3D modelling space. The beam dimensions were set to 1065 mm × 110 mm × 100 mm. Two lines were drawn to represent supports in a three-point bending test, which were positioned 132.5 mm from each edge to give an effective beam span of 800 mm. A central line was drawn to indicate the applied line load.

Material Properties. The input material properties of plain concrete were a density of 2.4×10^{-5}, Young's modulus of 14,176 MPa, and Poisson's ratio of 0.2. The yield stress was set to 14.438, with a plastic strain of 0. The maximum principal stress in *Maxps Damage* was set to 6.53 with a displacement of failure in damage evolution of 0.45. A homogeneous solid section was created and assigned to the entire beam. The material properties, including compressive strength (36.2 MPa), modulus of elasticity (25.4 GPa), and density (2400 kg/m³), were adopted from [27]. These were obtained via standard 150 mm cube compressive tests as per ASTM C39. This ensures consistency between the experimental fatigue data and the numerical modeling parameters.

Assembly. An instance was created from the part with a dependent instance type. This module was used to prepare the model for subsequent modules.

Step Creation. A static general procedure step was created with a time period of 50 s and a maximum of 10,000 increments. The initial minimum and maximum increment sizes were set to 0.1, 0.01, and 1, respectively, to ensure accuracy.

Interaction. A reference point was defined at the midpoint of the load line. A rigid body constraint was created to link the load line to the reference point to constrain the motion accurately.

Load Application. The load module was used to define a concentrated force based on cyclic loading data. The load was calculated using the following basic flexural mechanics equation (Equation 1):

$$P = \frac{2 \cdot B \cdot H^2 \sigma_{bend,max}}{3 \cdot S \cdot \sigma_{bend,max} \cdot 0.425} \tag{1}$$

A sinusoidal amplitude function was applied to simulate cyclic loading. The total time span was set for the simulation. The circular frequency, ω was calculated as $\omega = 2\pi f$ with $f = 30$ Hz. The initial amplitude was $\sigma_{bend,max} \times 0.575$ with $B = \sigma_{bend,max} \times 0.425$. The starting time was 0. To apply the sinusoidal amplitude, A was set to 0, and a value was assigned to B to account for the sine component (Figures 1 and 2). Boundary conditions were set to simulate the supports, ensuring immobility (Figure 3).

Table 1. Percentage of static ultimate strength values.

Ultimate Strength (%)	Maximum Flexural Stress (MPa)
74.6	4.870
70.0	4.568
68.9	4.497
61.2	3.997
52.5	3.426
35.0	2.286

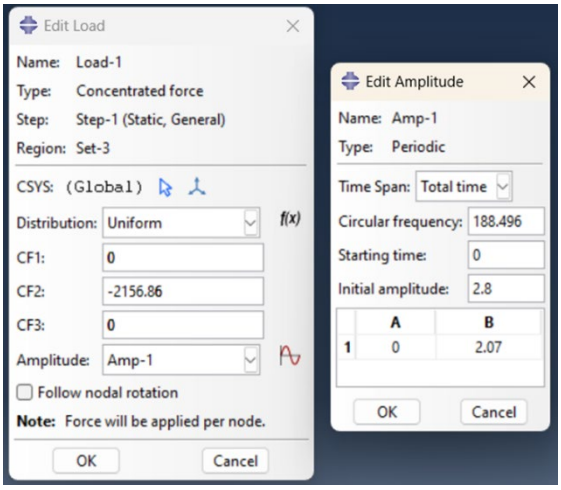

Figure 1. Values of load and amplitude input into Abaqus.

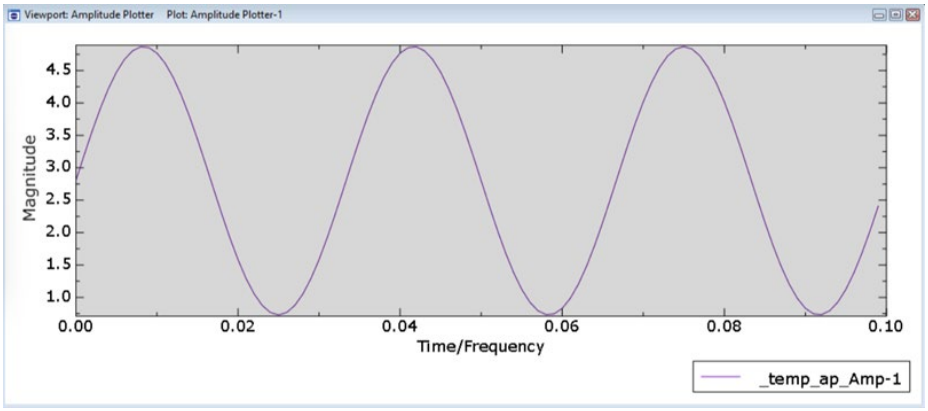

Figure 2. Amplitude plotter after values of *A* and *B* are entered.

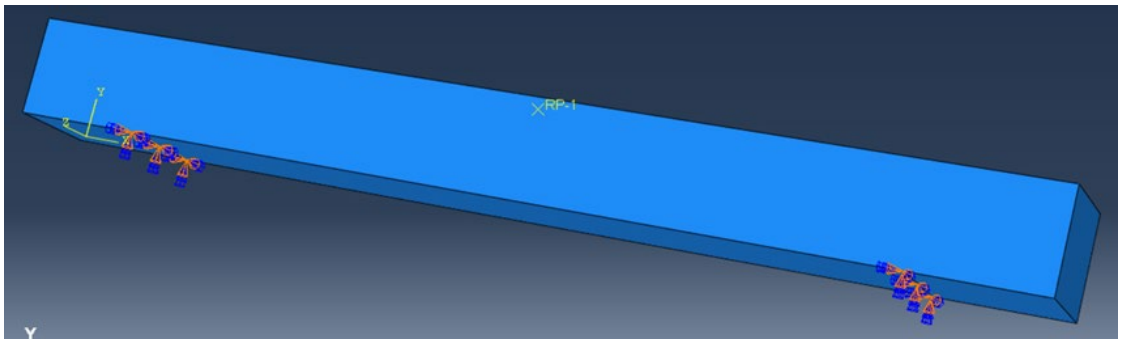

Figure 3. Model after the boundary conditions are set.

Meshing. The model was meshed using global seeds, with the mesh size adjusted to determine accuracy. The meshing process involved selecting an appropriate global size and meshing the part.

Job Submission. A new job was created and submitted for simulation. The processor count was set to 6 or 8, depending on the computational capacity.

Visualization. Results were viewed in the visualization module, displaying the output data and deflected model. Damage severity was indicated by a colour gradient from blue to red.

Validation. Mesh convergence was analysed by varying the mesh size (8, 10, 12, 14, 15, 20, 25, and 30 mm) to determine the optimal size for accurate results. The validated model, which showed the smallest percentage difference from experimental data, was used for further stress simulations. This approach ensured the model's reliability and efficiency, allowing the generation of comprehensive data for probabilistic modelling.

3.3 Enhancement of S–N Curve Through Probabilistic Models

The probabilistic model developed for predicting the fatigue life of plain concrete beams integrates data from experiments and finite element models. The analysis, using 14 data points of stress (S) and cycles to failure (N), was conducted in Microsoft Excel. Stress and cycles to failure data were first transformed using natural logarithms to linearize their relationship. Regression analysis yielded the slope (a) and intercept (b) for the S–N equation (Equation 2):

$$S = aN^b \tag{2}$$

where the parameters were determined as in Equations (3) and (4):

$$b = \frac{n\sum(\ln(N)\cdot\ln(S)) - \sum(\ln(N))\cdot\sum(\ln(S))}{n\sum(\ln(N)^2) - (\sum(\ln(N)))^2} \tag{3}$$

$$\mathrm{Ln}(a) = \frac{\sum(\ln(S)) - b\sum(\ln(N))}{n} \tag{4}$$

These values enabled the cycles to failure to be estimated at different stress levels and probabilities using the exponential distribution (Equation 5):

$$N_\mu = \left(\frac{S}{a}\right)^{\frac{1}{b}} \tag{5}$$

The rate parameter (λ) was calculated as in Equation (6):

$$\lambda = \frac{1}{N_\mu} \tag{6}$$

To estimate cycles to failure at different probabilities, the formula as in Equation (7):

$$F(x;\lambda) = 1 - e^{-\lambda x} \tag{7}$$

was used, where x represents the estimated number of cycles to failure and λ the rate parameter. By setting the probability at 99%, the model determined the cycles for failure. The resulting S–N curve graphically depicts stress versus estimated cycles to failure at various probabilities, providing insight into the model's predictive capability, complemented by a trendline and R^2 value for fit assessment.

4. RESULTS AND DISCUSSION

This section discusses the enhanced S–N curve developed through probabilistic modelling of experimental and finite element data.

4.1 Construction and Visualization of the Logarithmic S-N Curve

The experimental fatigue life data for the plain concrete beams reveal a highly nonlinear stress–cycle relationship, reinforcing the well-documented fatigue behaviour of quasi-brittle materials. As shown in Table 2, a dramatic reduction in fatigue life occurs as the stress increases. At 4.870 MPa (74.6% of the ultimate flexural strength), failure occurs in just 1,102 cycles, indicating extremely rapid deterioration due to high-energy cyclic loading and aggressive microcrack propagation. This is consistent with previous findings suggesting that when the stress amplitude exceeds 70% of the ultimate strength, fatigue failure occurs, predominantly due to the unstable coalescence of microcracks, leading to brittle fracture [29].

Conversely, at 2.286 MPa (35.0% of ultimate strength), the fatigue life extends to 30 million cycles, highlighting the significant stress dependence of concrete fatigue performance. This extreme disparity in failure cycles between high- and low-stress conditions underscores the critical influence of stress amplitude in determining fatigue life, a phenomenon often overlooked in deterministic fatigue models. Although the conventional S–N curve assumes a singular mathematical trend to predict fatigue life, these results clearly indicate its limitations, as fatigue failure varies significantly at lower stress levels due to the stochastic nature of crack nucleation and growth [6].

The logarithmic S–N curve (Figure 4) provides a more comprehensive visualization of the stress–life correlation. The high coefficient of determination (R^2 = 0.9893) suggests that a power-law function effectively captures the overall fatigue trend. However, this statistical fit does not fully capture the significant dispersion in experimental data arising from intrinsic material heterogeneity, environmental variations, and unquantifiable microstructural defects [13]. This highlights a critical limitation of traditional fatigue models, which fail to integrate probabilistic uncertainty, which can lead to miscalculations in fatigue life estimations.

4.2 Mesh Convergence and Validation

The reliability of any finite element model hinges on mesh convergence, ensuring computational predictions remain independent of element size. As detailed in Table 3, a comprehensive mesh convergence study determined the optimal element density for accurate stress computation in Abaqus. The results reveal that both excessively fine and coarse meshes introduce numerical inaccuracies, underlining the need for an optimized balance. The finest mesh (8 mm, 24,388 elements) yielded a maximum principal stress of 5.305 MPa, exceeding the experimental benchmark of 4.870 MPa, suggesting the presence of artificial stress concentrations induced by excessive discretization [30].

Table 2. Experiment data of plain concrete beam fatigue test.

% Ultimate flexural strength (MPa)	Maximum flexural stress (MPa)	Cycles to failure
74.6	4.870	1,102
70.0	4.568	8,845
68.9	4.497	17,464
61.2	3.997	191,573
52.5	3.426	5,533,659
35.0	2.286	30,000,000

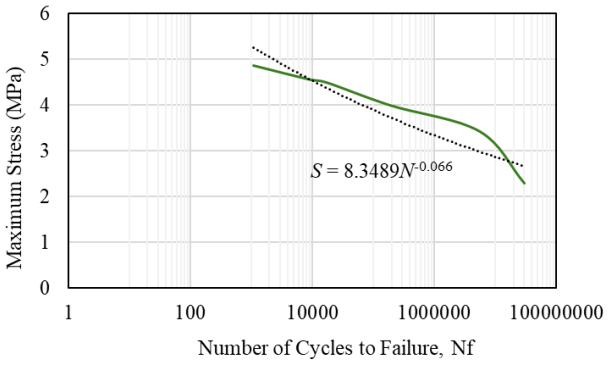

Figure 4. S-N curve plotting from the experiment.

Table 3. Data for mesh convergence obtained from Abaqus.

Mesh size (mm)	No. of elements	Results	Max. principal stress (MPa)
8	24,388	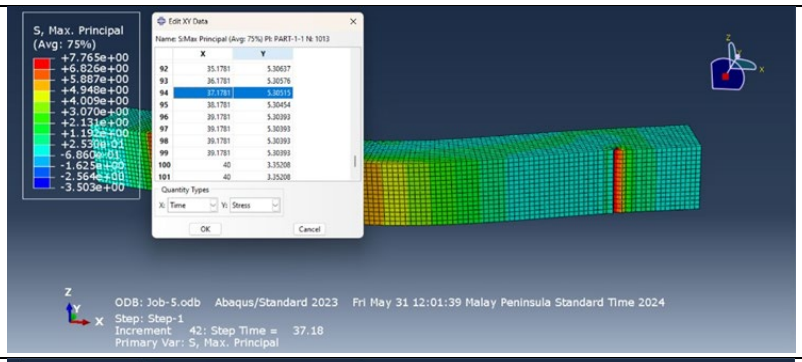	5.305
10	11,660	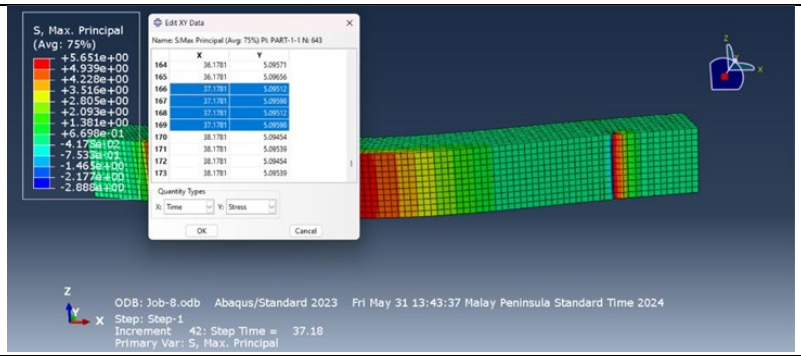	5.096
12	6,408	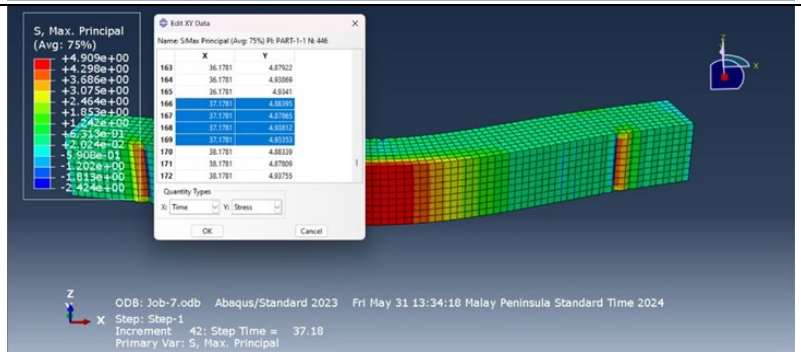	4.909
14	4,256	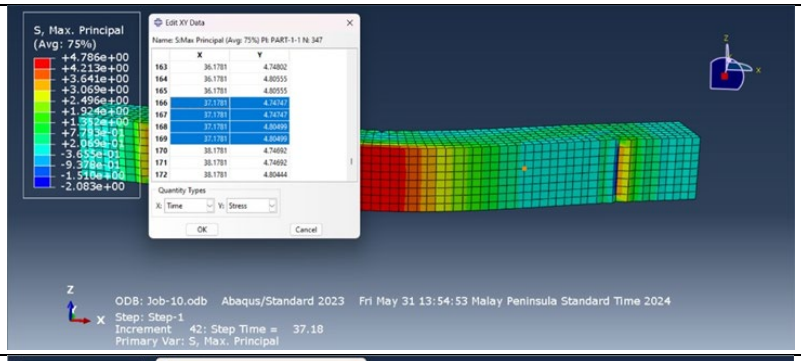	4.776
15	3,528	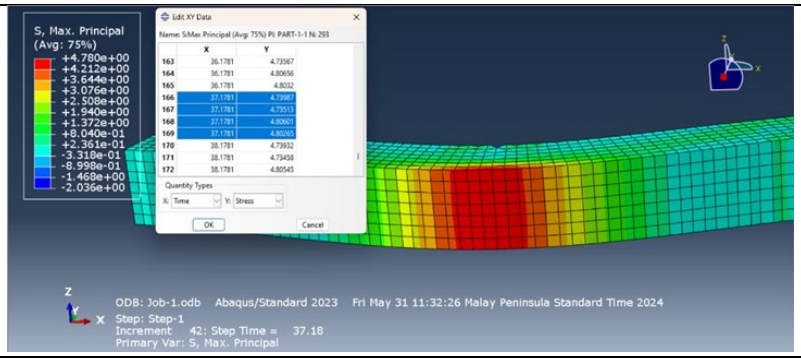	4.771

20	1,620	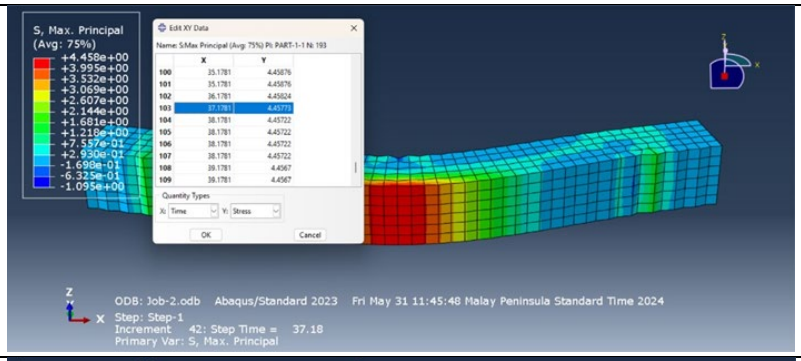	4.458
25	672	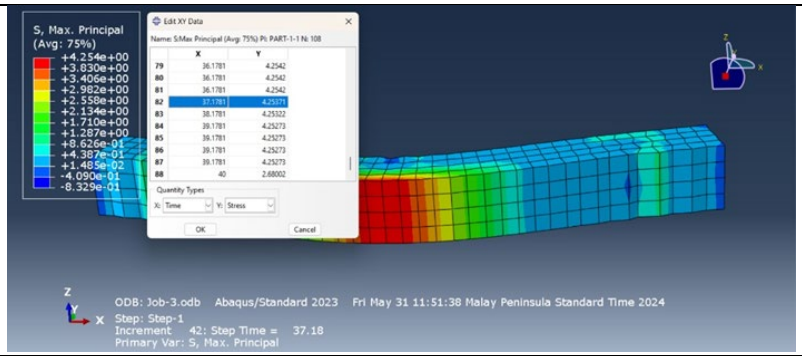	4.254
30	432	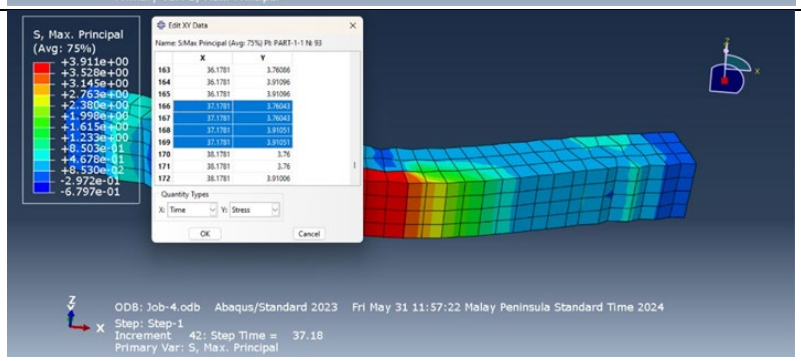	3.835

In contrast, a coarse mesh (30 mm, 432 elements) underestimated the maximum principal stress at 3.835 MPa, demonstrating that insufficient discretization fails to capture the actual stress distribution accurately. The mesh convergence trend derived from Table 3 is illustrated in Figure 5, which shows the variation of maximum principal stress with mesh refinement. As evident, convergence is achieved at a mesh size of 12 mm, corresponding to a principal stress of 4.909 MPa, closely matching experimental data. The mesh convergence analysis is presented in Table 3, which lists the mesh size, number of elements, and corresponding maximum principal stress. Figure 5 graphically illustrates the relationship between mesh density and computed stress, demonstrating convergence near a mesh size of 12 mm. This resolution achieves an optimal balance between computational cost and accuracy, aligning with the experimental benchmark of 4.87 MPa. Very fine meshes often lead to increased computational cost without proportionally improving accuracy, while coarse meshes under-represent stress gradients. Intermediate resolutions, such as the 12 mm mesh (yielding 6408 elements), offer a practical balance between accuracy and efficiency, providing results within 0.8% of the experimental benchmark. Hence, intermediate resolutions are therefore most effective for achieving reliable yet computationally feasible results [31]. This confirms that over-refinement introduces computational inefficiencies without increasing accuracy, while overly coarse meshes lead to oversimplified approximations. Intermediate resolutions are therefore most effective [32]. The validated FEA model ensures numerical consistency, enabling the generation of additional stress–life data points to refine the S–N curve analysis.

4.3 Integration of Probabilistic Modelling to Address Deterministic Limitations

To enhance fatigue life predictions, probabilistic modelling was applied using exponential distribution analysis. This approach accounts for the inherently stochastic nature of fatigue failure, where material heterogeneity, environmental influences, and loading variability introduce significant uncertainties [33]. The probabilistic S–N curve was enhanced by integrating additional data points obtained from FEA simulations, increasing the dataset to 14 observations (Table 3). A fundamental flaw of deterministic fatigue models is their inability to incorporate the stochastic nature of material failure. Concrete is inherently non-homogeneous, containing randomly distributed microvoids, aggregate–matrix interfaces, and pre-existing microcracks, which cause significant variability in fatigue life even under identical loading conditions [34]. A probabilistic fatigue model incorporating exponential distribution analysis was therefore developed to overcome this limitation to account for uncertainty in fatigue failure predictions.

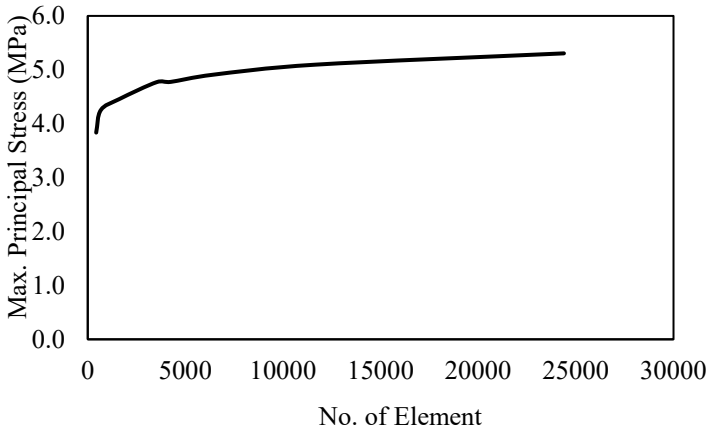

Figure 5. Mesh convergences in FEA.

Table 4. Data of plain concrete beam fatigue test from experiment and Abaqus.

Stress (*S*)	Cycles to failure (*Nf*)	Stress (*S*)	Cycles to failure (*Nf*)
2.286	30,000,000	3.997	191,524
2.368	26,567,010	4.056	165,420
2.589	20,191,920	4.339	17,465
3.14	11,818,650	4.497	15,845
3.426	5,533,560	4.568	8,855
3.598	3,999,000	4.685	4,985
3.606	2,764,929	4.870	1,115

The transformation of all experimental and numerical fatigue data into natural logarithm (*ln*) form (Table 4) facilitated the regression-based derivation of the fatigue equation (Equation 8):

$$S = 3488N^{-0.0647} \tag{8}$$

This equation characterizes the inverse exponential relationship between applied stress and fatigue life. However, unlike deterministic models, which rely on singular predictive values, the probabilistic approach enables failure cycle estimation across probability thresholds (e.g., 99%, 80%, 50%, and 20%), as detailed in Tables 4–10.

The results highlight a crucial distinction. At the low stress of 2.285 MPa, the predicted number of cycles to failure ranges from 2.27 billion (99% probability) to 110 million (20% probability), a vast spread in uncertainty. This indicates the high sensitivity of fatigue resistance to microstructural defects and environmental effects in the low-stress, long-life domain [35]. In contrast, at the high stress of 4.870 MPa, the variability is substantially reduced, with the predicted failure cycles ranging from 19,055 (99% probability) to 923 cycles (20% probability). This suggests that high-stress fatigue failure is primarily governed by deterministic factors such as macroscopic crack propagation, with reduced influence from material randomness [2].

The 14 data points, including the eight additional data points from the model, were used to create a more comprehensive S–N curve. Figure 5 illustrates this curve using logarithmic *x*- and *y*-axes. The equation of the trendline and the R^2 value are also given, providing a clear depiction of the relationship and the model fit.

4.4 Enhancement of S–N Curve Through Probabilistic Models

The deterministic approach to fatigue life prediction, which relies solely on empirical S–N curves, has long been recognized as insufficient for capturing the inherent variability and uncertainty in material failure. Plain concrete, in particular, is highly heterogeneous, with microcracks, voids, and interfacial flaws introducing significant stochastic influences on its fatigue behaviour. These variations lead to a wide scatter in experimental fatigue data, making conventional deterministic models unreliable for long-term structural performance assessment. To address this limitation, a probabilistic approach was integrated into the fatigue analysis, allowing the statistical estimation of fatigue life across different failure probabilities.

A crucial step in the probabilistic analysis involved transforming all experimental and finite element data into their natural logarithm (*ln*) form, as shown in Table 5. This transformation serves two purposes: first, it linearizes the highly nonlinear S-N relationship, making it more amenable to regression analysis; second, it enables the use of probability-based fatigue models by establishing a log-normal distribution of fatigue life data. Unlike conventional deterministic equations, which assume a fixed life expectancy for a given stress level, probabilistic models recognize that fatigue life has a range of possible outcomes, with certain probabilities associated with each failure cycle count. This distinction is critical in real-world applications, where loading conditions, environmental factors, and material inconsistencies introduce significant deviations from theoretical predictions [1]. Using regression-based parameter estimation, the fatigue life equation was determined by Equation (8).

Table 5. Data from experiment and Abaqus in natural logarithm (ln) form.

Stress (S)	Cycles to failure (N_f)	ln (S)	ln (N)	ln (S) × ln (N)	ln (N)^2
2.286	30,000,000	0.8266	17.2167	14.2311	296.4150
2.368	26,567,010	0.8620	17.0952	14.7368	292.2452
2.589	20,191,920	0.9513	16.8208	16.0011	282.9391
3.14	11,818,650	1.1442	16.2852	18.6339	265.2074
3.426	5,533,560	1.2314	15.5263	19.1190	241.0673
3.598	3,999,000	1.2804	15.2016	19.4637	231.0873
3.606	2,764,929	1.2826	14.8325	19.0242	220.0038
3.997	191,523.6	1.3855	12.1628	16.8520	147.9329
4.056	165,420	1.4002	12.0162	16.8251	144.3901
4.339	17,465.34	1.4676	9.7680	14.3359	95.4133
4.497	15,845.34	1.5034	9.6706	14.5385	93.5211
4.568	8,855.34	1.5191	9.0888	13.8065	82.6058
4.685	4,985.34	1.5444	8.5143	13.1491	72.4926
4.870	1,115.343	1.5832	7.0169	11.1089	49.2371
	Σ	17.9818	181.2159	221.8260	2,514.5580

Table 6. Mean cycles to failure and rate parameter.

No	Stress (S)	Mean cycles to failure (N_μ)	Rate parameter (λ)	No	Stress (S)	Mean cycles to failure (N_μ)	Rate parameter (λ)
1	2.286	494,159,188.8	2.02364E-09	8	3.997	87,674.98743	1.14058E-05
2	2.368	285,693,584.6	3.50025E-09	9	4.056	69,910.59725	1.4304E-05
3	2.589	71,967,158.02	1.38952E-08	10	4.339	24,656.46789	4.05573E-05
4	3.140	3,650,086.811	2.73966E-07	11	4.497	14,197.48645	7.0435E-05
5	3.426	949,139.5276	1.05359E-06	12	4.568	11,137.57386	8.97862E-05
6	3.598	445,255.8793	2.2459E-06	13	4.685	7,534.852877	0.000132717
7	3.606	430,234.6027	2.32431E-06	14	4.870	4,137.808892	0.000241674

Next, a and b were calculated as $a = 8.3488$ and $b = -0.0647$, respectively, using the equations outlined in the methodology. Thus, the equation can be expressed as $S = 8.3488N^{-0.0647}$. The mean cycles to failure and the rate parameter for each stress level were then calculated (Table 6). The estimated number of cycles to failure at different probabilities was also determined, with the results summarized in Tables 7–10 and visualized in Figures 6 to 9. As in the previous graph, the x- and y-axes have a logarithmic scale, and the trendline also follows a logarithmic function. The R^2 value of 0.9893 indicates that the equation fits the data well.

The 99% probability threshold represents an extremely conservative failure estimate, ensuring that only 1% of structures exceed the predicted fatigue life. This level of conservatism is typically applied to ultra-critical infrastructure, such as nuclear containment structures, offshore oil platforms, and high-speed-railway bridges, where even a marginal probability of premature fatigue failure is unacceptable due to catastrophic safety and economic consequences.

As shown in Table 7, the estimated failure cycle count at 2.2855 MPa exceeds 2.27 billion cycles, reinforcing the idea that under prolonged cyclic exposure, low-stress conditions induce gradual fatigue degradation rather than abrupt failure. However, at 4.870 MPa, the fatigue life is only 19,055 cycles, demonstrating that at high stress levels, failure is deterministic rather than probabilistic, as fatigue damage progresses rapidly and predictably.

The S–N curve in Figure 6 has a steep slope at higher stress levels, highlighting that under extreme cyclic loading, the stochastic influence of microstructural variations diminishes. This suggests that at high stress amplitudes, fatigue failure is driven almost entirely by macroscopic fracture mechanics rather than random defect propagation. Consequently, for ultra-conservative design applications, engineers must ensure that operational stress remains well within the low-stress regime, where failure variability remains high, and structures can exhibit extended fatigue life beyond deterministic estimates.

Table 7. Estimated number of cycles to failure of plain concrete beam at 99% probability.

Stress (*S*)	Cycles to failure (*Nf*)
2.2855	2,275,687,163
2.368	1,315,667,578
2.589	331,421,011
3.14	16,809,270
3.426	4,370,949
3.598	2,050,479
3.606	1,981,304
3.997	403,758
4.056	321,950
4.339	113,547
4.4968	65,382
4.568	51,290
4.685	34,699
4.8703	19,055

Table 8. Estimated number of cycles to failure of plain concrete beam at 80% probability.

Stress (*S*)	Cycles to failure (*Nf*)
2.2855	795,318,533
2.368	459,806,087
2.589	115,826,673
3.14	5,874,588
3.426	1,527,581
3.598	716,612
3.606	692,436
3.997	141,107
4.056	112,517
4.339	39,683
4.4968	22,850
4.568	17,925
4.685	12,127
4.8703	6,660

Table 9. Estimated number of cycles to failure of plain concrete beam at 50% probability.

Stress (*S*)	Cycles to failure (*Nf*)
2.2855	342,525,049
2.368	198,027,703
2.589	49,883,833
3.14	2,530,047
3.426	657,893
3.598	308,628
3.606	298,216
3.997	60,772
4.056	48,458
4.339	17,091
4.4968	9,841
4.568	7,720
4.685	5,223
4.8703	2,868

Table 10. Estimated number of cycles to failure of plain concrete beam at 20% probability.

Stress (*S*)	Cycles to failure (*Nf*)
2.2855	110,268,436
2.368	63,750,681
2.589	16,059,007
3.14	814,493
3.426	211,794
3.598	99,356
3.606	96,004
3.997	19,564
4.056	15,600
4.339	5,502
4.4968	3,168
4.568	2,485
4.685	1,681
4.8703	923

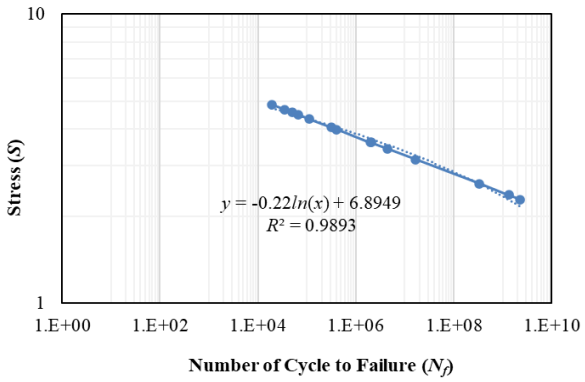

Figure 6. S–N curve for plain concrete beam to fail at 99% probability.

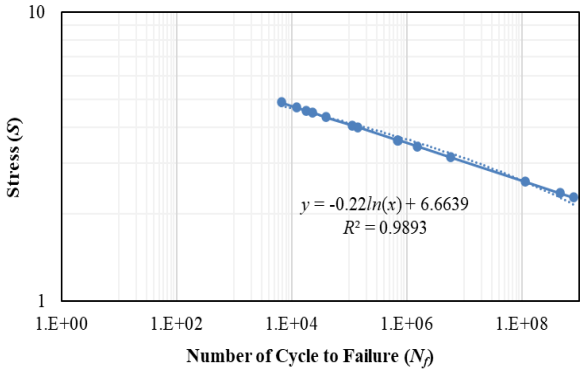

Figure 7. S–N curve for plain concrete beam to fail at 80% probability.

The 80% failure probability estimate provides a balance between safety and material efficiency, ensuring that most structures (80%) fail within the predicted fatigue cycles. This probability level is suitable for bridge decks, offshore wind turbine foundations, and high-rise buildings, where fatigue performance is critical but excessive conservatism could lead to unnecessarily high material costs.

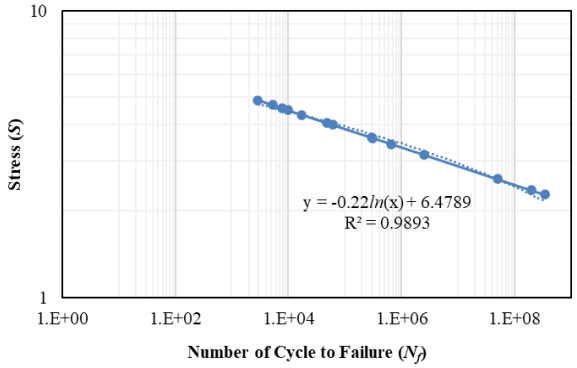

Figure 8. S–N curve for plain concrete beam to fail at 50% probability.

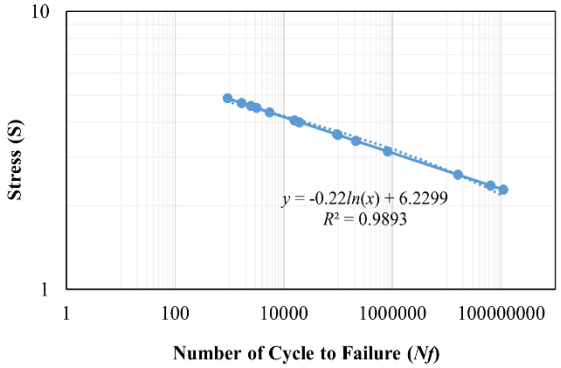

Figure 9. S–N curve for plain concrete beam to fail at 20% probability.

From Table 8, the estimated fatigue life at 2.2855 MPa is 795 million cycles, indicating that even with moderate safety margins, low-stress applications cannot be assumed to be fatigue-resistant indefinitely. At 4.870 MPa, the fatigue life reduces to 6,659 cycles, highlighting the need for strict fatigue performance limits in high-stress applications. The S–N curve in Figure 7 has a less steep slope than the 99% failure probability curve, indicating that at this probability level, failure variability remains substantial, particularly in the mid-stress regime. This suggests that for real-world high-risk infrastructure, engineers cannot rely on single deterministic values but must instead design structures within stress thresholds that consider long-term probabilistic fatigue behaviour. The 50% failure probability estimate corresponds to the median fatigue life expectation, making it a crucial reference for performance-based maintenance scheduling. This probability level is widely used in railway engineering, industrial flooring systems, and marine infrastructure, where long-term fatigue performance must be balanced against economic and operational constraints.

According to Table 9, at 2.2855 MPa, the estimated fatigue life is 342 million cycles, a considerable reduction from the 80% and 99% probability cases. This suggests that even in median fatigue life assessments, engineers must account for potential failure risks, particularly in high-cycle-loading environments. At 4.870 MPa, the predicted number of failure cycles falls to 2,868 cycles, confirming that structures subjected to elevated stress require continuous monitoring to prevent fatigue-induced failure [36]. The S–N curve in Figure 8 reveals consistent power-law decay, indicating that median probability fatigue behaviour is predictable within certain stress ranges. This reinforces the idea that deterministic models alone cannot fully capture fatigue life variability and that integrating probabilistic methods into structural health monitoring strategies is essential.

At the 20% failure probability threshold, the model provides a lower-bound fatigue life projection, indicating that only 20% of structures fail within the predicted number of cycles, while 80% exceed this lifespan. This probability level is particularly useful for non-critical structures, such as temporary formwork, scaffolding, and secondary road pavements, where high conservatism is not economically justified.

At 2.2855 MPa, the estimated failure cycle count is 110 million cycles (Table 10), highlighting that even in low-stress applications, fatigue failure remains a long-term concern. At 4.870 MPa, the failure cycle count drops to 923 cycles, confirming that under high-stress conditions, deterministic fracture mechanics dominate over stochastic influences. A particularly important consideration in long-life fatigue design is the 10-million-cycle fatigue limit observed in some studies. Plain concrete in certain conditions exhibits a fatigue threshold of approximately 10 million cycles, meaning that beyond this limit, further cyclic loading does not necessarily lead to immediate failure [36]. In the context of this study, the probabilistic analysis confirms that at stress levels below about 3 MPa, there is a substantial probability that the structure will exceed the 10-million-cycle threshold as shown in Figure 9. This suggests that for low-stress, long-life applications, deterministic fatigue models are even less reliable and that probabilistic assessments should be prioritized to ensure accurate fatigue life predictions.

5. CONCLUSION

This study has developed a comprehensive fatigue life prediction framework for plain concrete by integrating experimental fatigue testing, FEA, and probabilistic modelling. The widely used deterministic S–N curve approach was shown to be insufficient in capturing the inherent variability and stochastic nature of fatigue failure in concrete structures. To address this limitation, probabilistic failure models were employed to estimate fatigue life across multiple confidence levels, providing a realistic and risk-based approach to fatigue assessment. The results indicate that fatigue failure in plain concrete is not governed by a single deterministic value, but rather by a statistical distribution of possible failure cycles significantly influenced by stress levels, material heterogeneity, and microstructural imperfections.

A key finding of this research is the strong dependence of fatigue life on stress amplitude, where an increase in stress drastically reduces the number of cycles to failure. Finite element simulations, validated through mesh convergence studies, provided accurate stress estimations, confirming the reliability of the computational approach in predicting structural behaviour under cyclic loading. However, the deterministic fatigue life equation derived from regression analysis, $S = 8.3488N^{-0.0647}$,

while statistically significant (R^2 = 0.9893), was found to be insufficient for robust fatigue life prediction due to its failure to incorporate probabilistic uncertainty. By applying exponential probability distributions, the study quantified failure probabilities at 99%, 80%, 50%, and 20% confidence levels, enabling engineers to assess fatigue risk with greater precision.

The findings also reinforce the importance of considering the fatigue endurance limit in structural design, particularly in long-life applications. The 10-million-cycle fatigue threshold identified in the literature suggests that at stress levels below approximately 3 MPa, concrete structures can exhibit indefinite fatigue resistance under controlled conditions. The probabilistic analysis further supports this, demonstrating that at lower stress levels, there is a high probability of exceeding 10 million cycles, although long-term environmental degradation factors such as corrosion, freeze–thaw effects, and creep must still be considered. These insights highlight the need to incorporate probabilistic endurance thresholds into fatigue design standards, rather than relying on overly conservative deterministic assumptions.

ACKNOWLEDGEMENTS

The authors extend their heartfelt gratitude to Universiti Teknologi Malaysia (UTM) for providing the resources and facilities that enabled the successful execution of this research. They also express their deep appreciation to the Malaysian Ministry of Higher Education (MoHE) for its financial support under research grant PY/2023/02180 (FRGS/1/2023/TK06/UTM/02/12) and to Universiti Teknologi Malaysia for funding through the Fundamental Research Grant Scheme PY/2024/00774 (Q.J130000.3822.23H88). These contributions were instrumental in ensuring the successful completion of this research.

DECLARATION OF CONFLICTING INTERESTS

The authors declare no potential conflicts of interest with respect to the research and publication of this article.

REFERENCES

[1] H. Chen, Z. Sun, Z. Zhong and Y. Huang, Fatigue factor assessment and life prediction of concrete based on Bayesian regularized BP neural network, *Materials*, 15(13), 2022, 4491.
[2] N. Oneschkow, T. Scheiden, M. Hüpgen, C. Rozanski and M. Haist, Fatigue-induced damage in high-strength concrete microstructure, *Materials*, 14(19), 2021, 5650.
[3] F. Z. Kachkouch, C. C. Noberto, L. F. D. A. L. Babadopulos, A. R. S. Melo, A. M. L. Machado, N. Sebaibi, F. Boukhelf and Y. El Mendili, Fatigue behavior of concrete: A literature review on the main relevant parameters, *Construction and Building Materials*, 338, 2022, 127510.
[4] D. R. Renju and M. S. Keerthy, A review on fatigue life prediction of plain concrete, *IOP Conference Series: Materials Science and Engineering*, 936(1), 2020, 012026.
[5] H. Rana and A. Ibrahimbegovic, A hybrid physics-informed and data-driven approach for predicting the fatigue life of concrete using an energy-based fatigue model and machine learning, *Computation*, 13(3), 2025, 61.
[6] H. Chen, Z. Sun, X. Zhang and J. Fan, Tensile fatigue properties of ordinary plain concrete and reinforced concrete under flexural loading, *Materials*, 16(19), 2023, 6447.
[7] M. S. A. Shah, N. Noor, A. B. H. Kueh and M. N. Tamin, A review on the application of the theory of critical distance towards concrete, *MATEC Web of Conferences*, 250, 2018, 03001.
[8] S. Yang, Special issue on fatigue, performance, and damage assessments of concrete, *Applied Sciences*, 14(5), 2024, 1845.
[9] C. Qin, X. Dong, B. Wu, L. Cai, S. Wang and Q. Xia, Fatigue damage analysis of plain and steel fiber-reinforced concrete material based on a stiffness degradation microplane model, *Frontiers in Materials*, 11, 2024, 1505295.
[10] E. F. Félix, R. Carrazedo and E. Possan, Fatigue life of concrete: Experimental study on the influence of loading conditions and material strength, *Revista Alconpat*, 12(1), 2022, 1-15.
[11] Z. Zhang and Y. Huo, Fatigue life prediction model of FRP–concrete interface based on gene expression programming, *Materials*, 17(3), 2024, 690.
[12] Z. Fan and Y. Sun, Detecting and evaluation of fatigue damage in concrete with industrial computed tomography technology, *Construction and Building Materials*, 223, 2019, 794-805.
[13] I. N. Yadav and K. B. Thapa, Fatigue damage model of concrete materials, *Theoretical and Applied Fracture Mechanics*, 108, 2020, 102578.
[14] S. R. Kasu, S. Deb, N. Mitra, A. R. Muppireddy and S. R. Kusam, Influence of aggregate size on flexural fatigue response of concrete, *Construction and Building Materials*, 229, 2019, 116922.
[15] H. Becks and M. Classen, New insights into the load sequence effect: Experimental characterization and incremental modeling of plain high-strength concrete under mode II fatigue loading with variable amplitude, *International Journal of Fatigue*, 185, 2024, 108334.
[16] L. Zhang, B. Jiang, P. Zhang, H. Yan, X. Xu, R. Liu, J. Tang and C. Ren, Methods for fatigue-life estimation: A review of the current status and future trends, *Nanotechnology and Precision Engineering*, 6(2), 2023, 025001.
[17] X. Wei, D. A. Makhloof and X. Ren, Analytical models of concrete fatigue: A state-of-the-art review, *CMES-Computer Modeling in Engineering & Sciences*, 134(1), 2022, 9-34.
[18] A. M. Alshoaibi and Y. A. Fageehi, Advances in finite element modeling of fatigue crack propagation, *Applied Sciences*, 14(20), 2024, 9297.
[19] J. Sun, Z. Ding and Q. Huang, Corrosion fatigue life prediction for steel bar in concrete based on fatigue crack propagation and equivalent initial flaw size, *Construction and Building Materials*, 195, 2019, 208-217.

[20] O. Alrayes, C. Könke, E. T. Ooi and K. M. Hamdia, Modeling cyclic crack propagation in concrete using the scaled boundary finite element method coupled with the cumulative damage-plasticity constitutive law, *Materials*, 16(2), 2023, 863.
[21] S. Rastayesh, A. Mankar, J. D. Sørensen and S. Bahrebar, Development of stochastic fatigue model of reinforcement for reliability of concrete structures, *Applied Sciences*, 10(2), 2020, 604.
[22] J. Velarde, C. Kramhøf, A. Mankar and J. Sørensen, Uncertainty modeling and fatigue reliability assessment of offshore wind turbine concrete structures, *International Journal of Offshore and Polar Engineering*, 29(2), 2019, 165-174.
[23] B. Ge and S. Kim, Probabilistic service life prediction updating with inspection information for RC structures subjected to coupled corrosion and fatigue, *Engineering Structures*, 238, 2021, 112260.
[24] J. Wu, B. Zhang, J. Xu, L. Jin and B. Diao, Probabilistic fatigue life prediction for RC beams under chloride environment considering the statistical uncertainty by Bayesian updating, *International Journal of Fatigue*, 173, 2023, 107680.
[25] J. Lee, C. H. Jeon, C. S. Shim and Y. J. Lee, Bayesian inference of pit corrosion in prestressing strands using markov chain monte carlo method, *Probabilistic Engineering Mechanics*, 74, 2023, 103512.
[26] J. Huang, S. Qiu and D. Rodrigue, Parameters estimation and fatigue life prediction of sisal fibre reinforced foam concrete, *Journal of Materials Research and Technology*, 20, 2022, 381-396.
[27] M. S. Ahmad Shah, A. B. H. Kueh, M. N. Tamin, J. H. J. Kim, M. A. Ab. Kadir, N. Yahaya and N. Md. Noor, Water–cement ratio on high-cycle fatigue in the theory of critical distances of plain concrete, *Iranian Journal of Science and Technology, Transactions of Civil Engineering*, 46(6), 2022, 4281-4290.
[28] Q. Zhang and L. Wang, Investigation of stress level on fatigue performance of plain concrete based on energy dissipation method, *Construction and Building Materials*, 269, 2021, 121287.
[29] P. Singh, *Experimental Studies on the Fracture and Fatigue Failure Processes Under Direct Tension in Quasi-Brittle Materials-Graphite and Concrete*, PhD Thesis, Indian Institute of Science, India, 2021.
[30] B. Sun and Z. Xu, An efficient numerical method for meso-scopic fatigue damage analysis of heterogeneous concrete, *Construction and Building Materials*, 278, 2021, 122395.
[31] A. Alañón, E. Cerro-Prada, M. J. Vázquez-Gallo and A. P. Santos, Mesh size effect on finite-element modeling of blast-loaded reinforced concrete slab, *Engineering with Computers*, 34, 2018, 649-658.
[32] A. Al-Saoudi, R. Al-Mahaidi, R. Kalfat and J. Cervenka, Finite element investigation of the fatigue performance of FRP laminates bonded to concrete, *Composite Structures*, 208, 2019, 322-337.
[33] E. C. Ferreira, P. Sotoudeh, G. Fiorillo and D. Svecova, The probabilistic fatigue life of plain concrete under low-frequency stress reversal loading, *Life-Cycle of Structures and Infrastructure Systems*, 2023, 3492-3499.
[34] R. L. Riyar, Mansi and S. Bhowmik, Fatigue behaviour of plain and reinforced concrete: A systematic review, *Theoretical and Applied Fracture Mechanics*, 125, 2023, 103867.
[35] H. L. Fu, H. S. Deng, Y. M. Wu, Y. B. Zhao and C. D. Xie, Low stress level and low stress amplitude fatigue loading simulation of concrete components containing cold joints under fatigue loading, *Applied Sciences*, 14(17), 2024, 7709.
[36] U. Karr, R. Schuller, M. Fitzka, A. Denk, A. Strauss and H. Mayer, Very high cycle fatigue testing of concrete using ultrasonic cycling, *Materials Testing*, 59(5), 2017, 438-444.